BOLLETTINO DI GEOFISICA TEORICA ED APPLICATA VOL. XXXVII, N. 148 - DECEMBER 1995

E. CARDARELLI [1], U. MASCIA [2], A. NERI [3] and S. PULEDDA [2]

SEISMIC 3D-TOMOGRAPHY WITH STATISTICAL CONSTRAINTS ON PILLARS OF THE COLISEUM, ROME

Abstract. In this work we present the results obtained on some pillars of the Coliseum in Rome using the statistical technique of 3D-tomographic inversion. This approach makes it possible to insert into the inversion process statistical a priori knowledge about the velocity field. The key aspect of the method is the ability to describe the form of the field without fixing any deterministic constraints; this is obtained by means of Markov (or Gibbs) statistics, the proper choice of parameters making it possible to describe a great variety of different fields, so the resulting method is quite general. Using this algorithm we obtained a great improvement in resolution compared to traditional methods without introducing any artefacts into the reconstruction, as we will show from the results obtained on some of the pillars of the Coliseum.

INTRODUCTION

It is known that in tomography an important requirement is to obtain a large number of independent ray-paths in order to get high resolution in the velocity field restoration. But this requirement conflicts with the economics of the survey, because the more the paths, the more the sources, so that a greater execution time is needed, with a notable increase in costs. Furthermore, in many cases the number of sources and receivers is limited by the particular configuration of the area. For these reasons, the number of paths is necessarily limited.

At this point, if we resort to classical tomographic methods, we have to compromise, and bound the total number of cells in such a way that the solution of the algorithm does not lead to artefacts without any physical meaning. This paper explains a method that, using techniques typical of statistical estimation, makes it possible to override part of these limitations, and presents some results in comparison with those obtained with traditional methods.

SOLUTION BY MEANS OF MAXIMUM "A POSTERIORI" PROBABILITY ESTIMATION

The key to the method explained in the following consists of taking into account the "a priori" information available about the velocity field - or rather about the slowness field - because, as said, the reconstruction problem to solve has a limited set of projections, so that we cannot get high resolution: the introduction of a feasible probabilistic model for the field under study allows one to overcome this obstacle.

Manuscript received, April 8, 1994; accepted, August 10, 1994.

[1] Dip. ITS, Area di Geofisica, Università "La Sapienza", Roma, Italy.

[2] Dip. InfoCom, Università "La Sapienza", Roma, Italy.

[3] III Università di Roma, Italy.

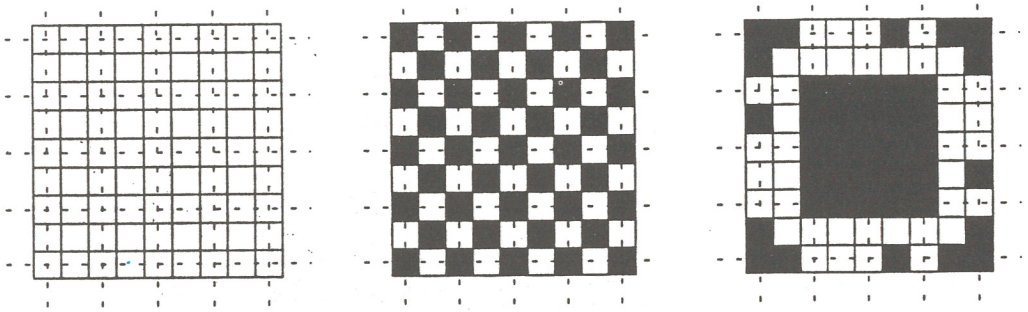

Fig. 1 - Example of a highly indeterminate tomographic reconstruction.

Prior information can be defined in this way: *the velocity (or slowness) field is composed of some connected regions, in which velocity varies gradually.*

In other words, we make the following assumptions:

- the investigated region is composed of several parts, each having its own characteristics, not varying much inside;

- the various parts are divided by rough discontinuities.

These conditions can be applied to some geological experiments when there are stratified formations, and in particular to the case of the pillars of the Coliseum, which we discuss. In other cases, the same algorithm can be employed but with different parameters.

Let us consider an illustrative example. Imagine 10 tomographic measurements on a region where cells can assume one of only two possible configurations ("black" or "white"), and choose a 9x9 lattice, giving thus 81 cells: it is a highly indeterminate situation, with a lot of possible ambiguities. For example, for the system of equations obtained from the measures, either Fig. 1b or Fig. 1c are exact solutions, and therefore both valid. Fig. 1c, however, shows a higher degree of connection, that is aggregated regions with similar properties, and so is nearer to the natural characteristics of the investigated spaces.

Now we have to introduce a procedure that rewards "aggregated" configurations rather than "dispersive" ones, since the first are more likely in nature than the others: this procedure is a probability measure.

A flexible stochastic model that answers to this need is given by Markov Random Fields (MRF).

Let $\boldsymbol{S}$ be a finite lattice; that is a set of cells, each one associated with a random variable X_S. The set of these variables forms the random field $\boldsymbol{X}_{\boldsymbol{S}}$. We say that $\boldsymbol{X}_{\boldsymbol{S}}$ is a MRF if the probability that any variable X_S assumes a certain value, given the values taken from all the other variables of the field, is equal to the probability conditioned only by some variables associated with a small number of cells near the one taken into consideration. This set of cells is the *neighborhood*, labelled ∂s. We will denote by $\underline{\boldsymbol{X}}_{S-s}$ the set of all random variables of the fields apart from X_S; and by $\underline{\boldsymbol{X}}_{\partial s}$ the set of random variables associated with the neighborhood of the cell s; finally, we denote the random variables with uppercases and their values with lowercases. With this notation the Markovianity property is:

$$Pr\{X_s=x_s \mid \underline{\boldsymbol{X}}_{S-s}=\underline{x}_{S-s}\}=Pr\{X_s=x_s \mid \underline{\boldsymbol{X}}_{\partial s}=\underline{\boldsymbol{x}}_{\partial s}\}\ . \tag{1}$$

The probability measure of interest in this problem is not directly $P(\underline{\boldsymbol{X}}=\underline{x})$, which takes into account generic "a priori" knowledge, but the conditional posterior distribution, where the constraint of the measures appears, and which is labelled as $P(\underline{\boldsymbol{X}}=\underline{x}/\underline{\boldsymbol{Y}}=\underline{y})$. Once we have found the particular expression of $P(\underline{\boldsymbol{X}}=\underline{x}/\underline{\boldsymbol{Y}}=\underline{y})$ for the problem under examination, the solution will be the configuration of the field with the higher "reward", that is the most likely one.

More properly, we are looking for the maximum a posteriori estimate (MAP):

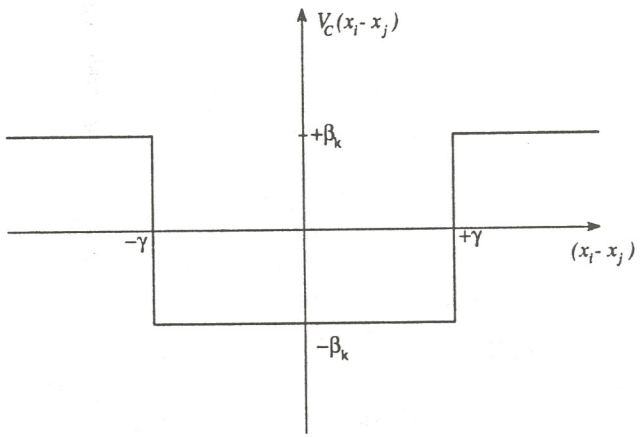

Fig. 2 - Potential function β (x_i, x_j) adopted.

$$\underline{\hat{x}}_{MAP} = arg \left(\max_{\underline{x}} \left\{ P\left(\underline{\mathbf{X}}=\underline{x} \mid \underline{\mathbf{Y}}=\underline{y}\right) \right\} \right) . \tag{2}$$

It is possible to show (Geman and Geman, 1984; Geman, 1988) that under the following assumptions:

1) the slowness field $\boldsymbol{X}$ is represented by MRF;

2) the relationship between the slowness and tomographic measures (data vector y), with the addition of a noise term (white Gaussian) is $\underline{y}=f(\underline{x})+\underline{w}$, with $\underline{w} : N(\underline{0}, \sigma_w^2 \boldsymbol{I})$; then the conditional posterior distribution is

$$P\left(\underline{\mathbf{X}}=\underline{x} \mid \underline{\mathbf{Y}}=\underline{y}\right) = \frac{1}{Z_p} \exp\left\{-U_p(\underline{x})\right\} ; \tag{3}$$

$$U_p(\underline{x}) = \frac{1}{T} U(\underline{x}) + \frac{1}{2\sigma_w^2} \left[\underline{y}-f(\underline{x})\right]^T \left[\underline{y}-f(\underline{x})\right] , \tag{4}$$

known in literature as the Gibbs distribution.

In the case of a perturbed solution where it is possible to use a linear approximation, eqn. (4) becomes

$$U_p(\underline{x}) = \frac{1}{T} U(\underline{x}) + \frac{1}{2\sigma_w^2} \left[\underline{y}-\mathbf{A}\underline{x}\right]^T \left[\underline{y}-\mathbf{A}\underline{x}\right] . \tag{4 bis}$$

Since Z_P is a normalizing constant, the MAP solution is also expressible as

$$\underline{\hat{x}}_{MAP} = arg \left(\min_{\underline{x}} U_P(\underline{x}) \right) . \tag{5}$$

Because of the high non-linearity of the problem, the extrema of eqn. (5) are localized by means of a stochastic relaxation algorithm called the Gibbs Sampler (Geman and Geman, 1984; Geman, 1988).

It is convenient to explain in detail the form of $U_P(\underline{x})$, which is composed of two terms. As a general rule, the smaller the addendum, the more likely the configuration $\underline{x}$, even though

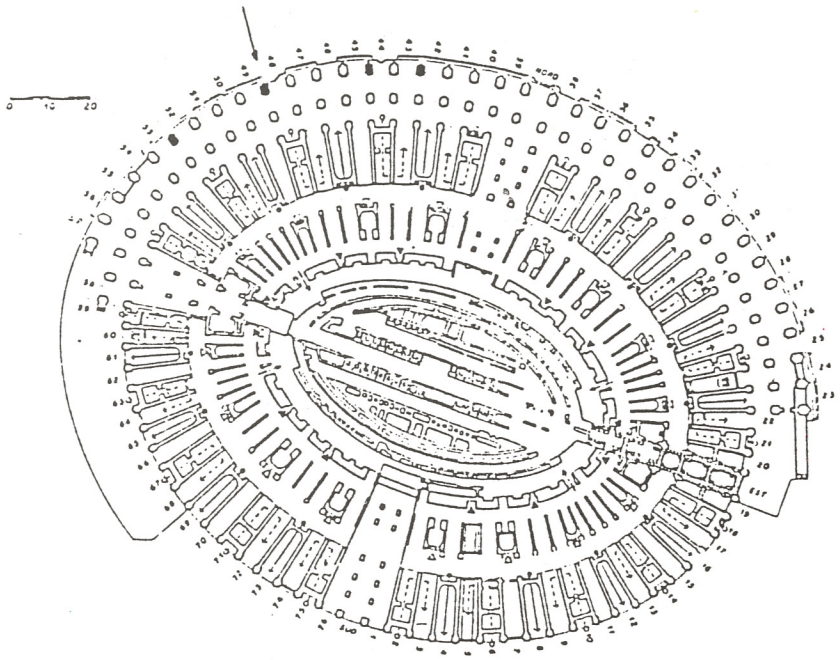

Fig. 3 - Coliseum Planimetry.

the MAP solution usually does not reach the absolute minimum for each addendum at the same time. The two multiplicative factors can be used, during the estimation procedure, to give more or less weight to the measures or to the selected slowness field model.

The second addendum evaluates the closeness of the field $\underline{\boldsymbol{X}}$ to the measures: if we had only this term, the solution would be the configuration with the minimum mean square error.

The first addendum is related to the selected stochastic model. It is called the *energy function*, and it is expressible in turn as sum of functions called *"potentials"*, which determine the existing connections between near cells. In particular, in the model that we adopted, we chose to take into consideration only correlations between pairs of adjacent cells over the co-ordinate and oblique directions, obtaining a satisfactory compromise between model generality and calculation complexity. However, it is better to confirm that $U(x)$ can take the more general form

$$U(\underline{x}) = \sum_{(i),\,(j)\,\epsilon S} \beta\,(x_i\,,\,x_j) \tag{6}$$

So $\beta\,(x_i, x_j)$ is null if cells (i) and (j) are not neighbours; otherwise it has a form set according to the physical properties to be represented. In our case, $\beta\,(x_i, x_j)$ has the form illustrated in Fig. 2: a two-valued function $(\pm\beta_k)$, according to whether the absolute value of the difference between values of the field in two adjacent cells is higher or lower than a threshold γ.

With this choice the following conditions hold:

- adjacent cells with values less distant than γ are "rewarded", because they bring a negative contribution to $U(\underline{x})$;

- the larger β_k, the more the rewards: so we can establish preferential directions for the aggregations, giving different β_k values to different directions;

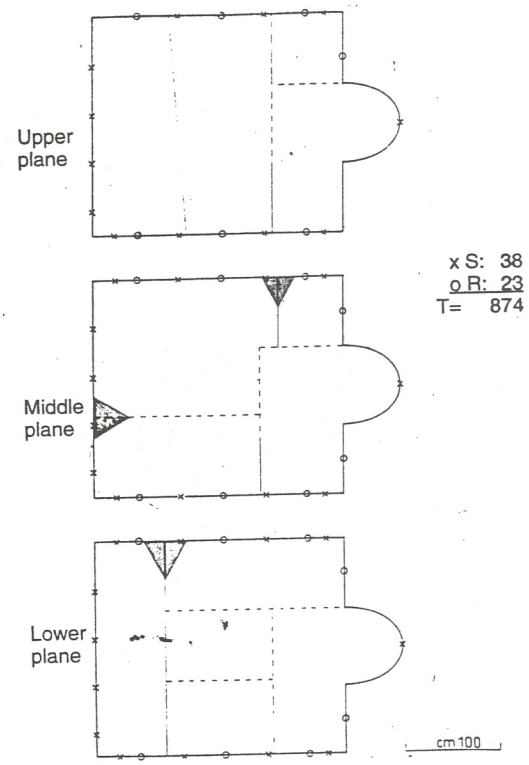

Fig. 4 - Receivers and sources geometry.

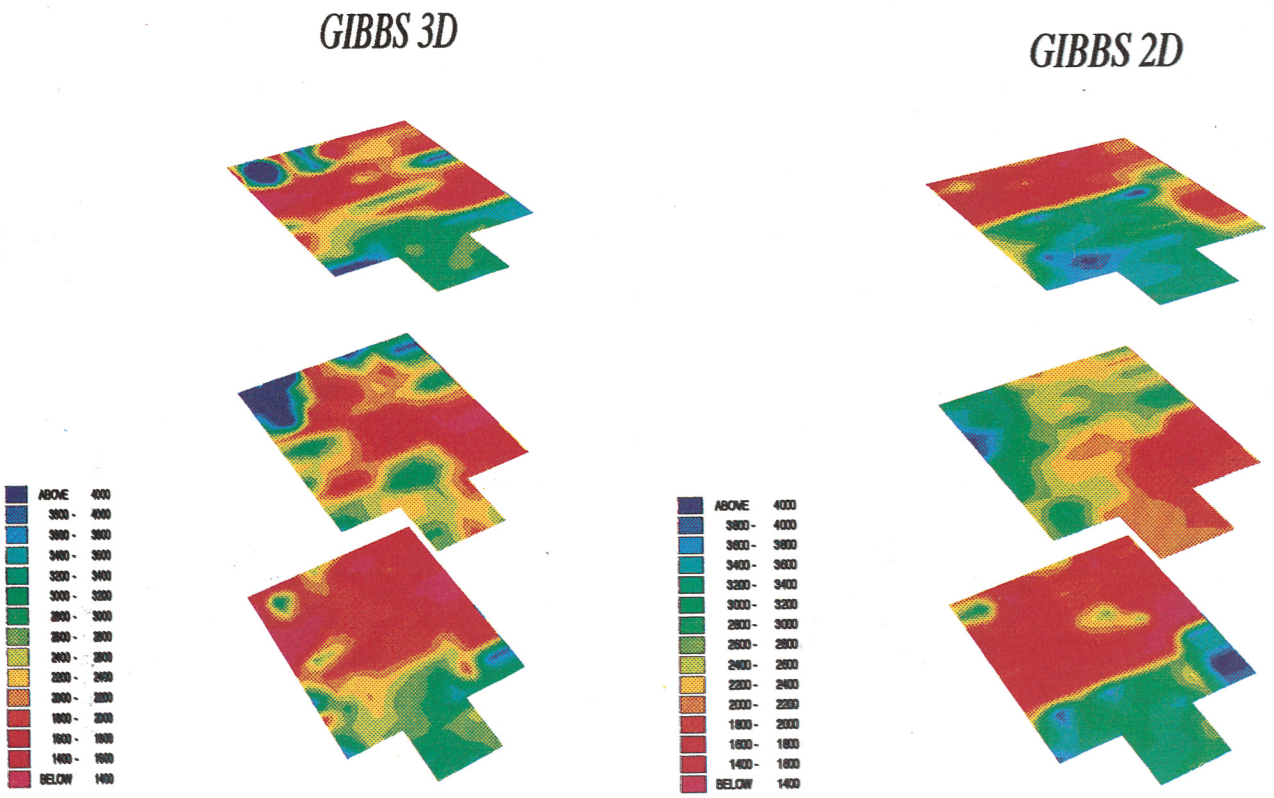

Fig. 5 - Statistical tomograph: 3D e 2D reconstructions.

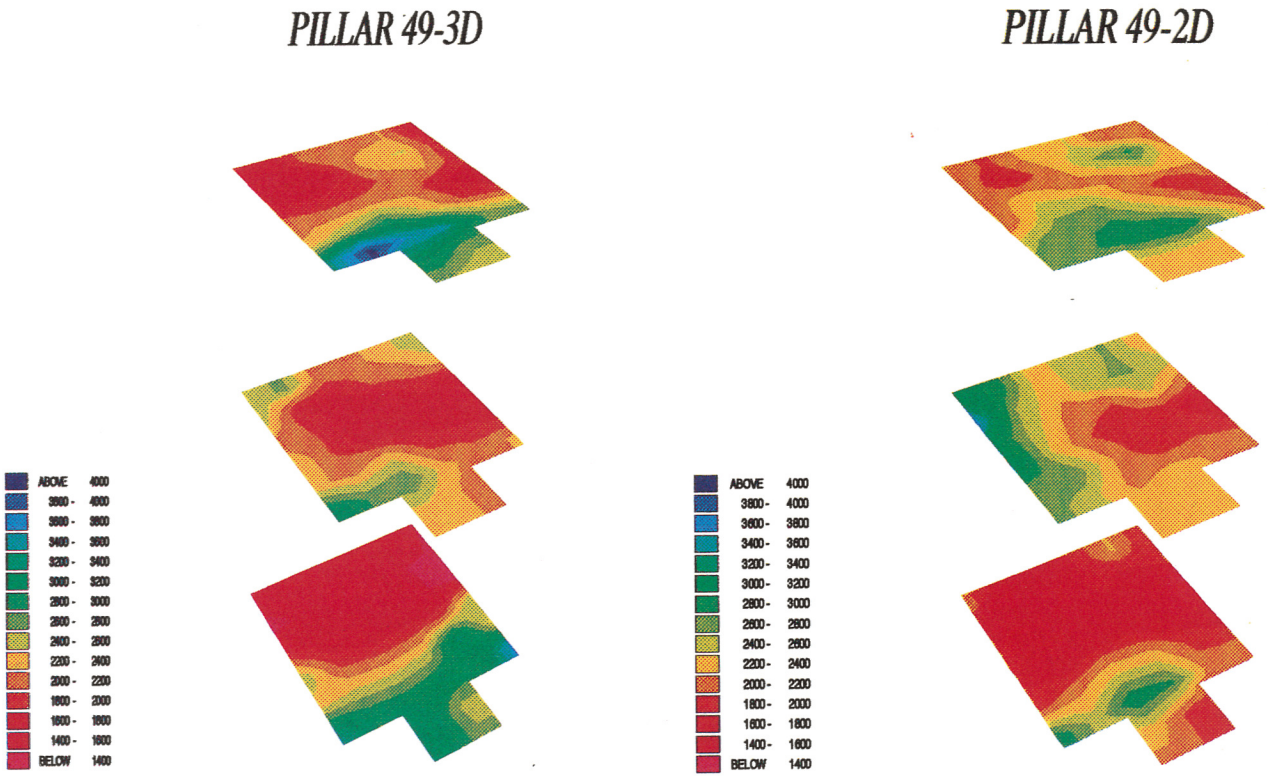

Fig. 6 - 3D reconstruction: comparison between statistical and LSQR tomograph.

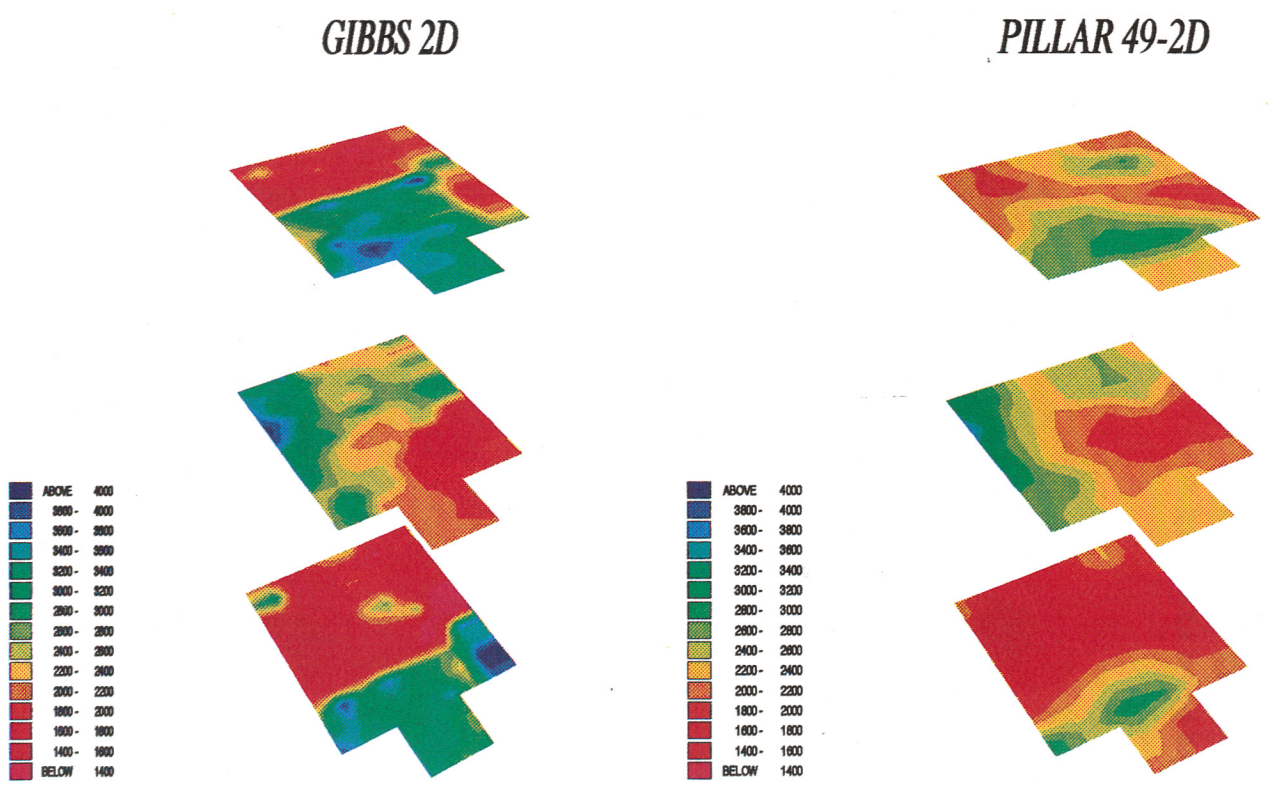

Fig. 7 - 2D reconstruction: comparison between statistical and LSQR tomograph.

- if the values of two cells are more distant than γ, they bring a constant contribution β_k, whatever their actual distance: this property encourages sharp discontinuities between near regions.

In the investigation of the Coliseum pillars, this choice for the shape of the potentials seemed appropriate, having to represent a volume composed of different blocks with distinctly outlined boundaries. In other contexts, where for example a gradual variation of the material properties must be represented, a smoother $\beta\ (x_i, x_j)$ could be employed.

The β_k values were chosen following heuristic considerations. The Coliseum pillars were built with superimposed blocks of regular shape: in the choice of β_k, we favoured the three co-ordinate directions, and particularly the horizontal directions over the vertical; whereas negative values were given to parameters referred to oblique directions.

In the tests carried out, we observed a low sensitivity of the solution to the actual values of β_k, which can vary over a wide range without significant changes in the reconstructed field; out of this range, the stochastic model gets the upper hand over the final results.

The problem of identification of the parameters values that match the model best to reality is crucial to get better results, and so a stochastic procedure to estimate the β_k values is under study.

TESTS ON THE COLISEUM PILLARS

In order to test the algorithm, we used a set of data previously recorded for another tomographic study on the Coliseum pillars (Cardarelli, 1995). That study was focused on four pillars of the lower ambulatory, which are denoted in the planimetry (Fig. 3) by the numbers 43-45-49-53; we focused our attention on pillar 49 because it was the most difficult to image. We then compared our results with those obtained in the other study (Cardarelli, 1995), using an algorithm based on LSQR (Paige and Saunder, 1982).

The data collection

We give now some notes on the data collection. For more details see Bernabini et al. (1990) and Cardarelli (1995).

A digital seismograph with 24 channels, and a time resolution of 24 μs, was used. Piezoelectric transducer were used as receivers, this choice was made to obtain the best SNR. The receivers were attached to the pillar with ceramic cement, in order to get the best conditions for transmission of elastic waves. There were 23 receivers (the number of free lines in the seismograph), and their locations were chosen to give the best coverage over the inspected section. A group of 30-40 acoustic sources were used on each pillar, and for each source the 23 arrival times were recorded. In such way we had 700-900 recorded data points.

A preliminary analysis allowed us to drop data that were not plausible for the following reasons:

- the line from the source to the receiver was not completely inside the pillar (on account of its irregular geometry);

- the noise of the recorded data did not allow recognition of the first arrival time, with sufficient precision;

- the arrival times were implausible for the pillar material.

After this first elaboration, we were left with 500-600 useful projections.

Results

We used, as explained, the data for pillar 49. In Fig. 4 it is possible to examine the position of sources and receivers on the three investigated sections.

We did a 3-D tomographic inversion on the whole section of the pillar, and a series of 3 2-D inversions on each plane (discarding the projection with the source in one plane and the receiver in another plane) corresponding to each level of travertine quoins, as was done in the previous work (Cardarelli, 1995), in order to show the preferential fracture direction.

Table - Numeric results.

PILLAR 49	Dimension of survey area: 225x329x204 [cm]	
	Statistical Tomograph	LSQR tomograph
Adopted division	9x14x3	6x9x3
Cell dimension	25x24x82 [cm]	37.5x38.5x82 [cm]
Mean error	39 [μs]	44 [μs]
Mean standard deviation (σ)	318 [μs]	334 [μs]
Ratio σ/mean measured time	0.274	0.288

The 2-D reconstructions obtained were compared with the 3-D reconstruction and with the 2-D reconstructions obtained with the LSQR algorithm. The results are shown in figures 5 to 7, which represent the velocity field by contouring. For a better comprehension of the results it is also useful to look at Fig. 4, which shows the fragmentation at each level in the quoins.

Comparison of the 3-D and 2-D reconstructions (Fig. 5) shows a substantial agreement in general structure but with some differences in details. These differences can be explained by fracture anisotropies, which disappear in the 3D reconstruction due to those rays which run in the same direction as the fracture. Moreover only three levels were chosen in the vertical direction because it was meaningless to have a resolution greater than the number of levels of quoins. However, this choice was not well suited to the statistical model, which needs a slighty larger number of divisions. All the same, we obtained a successful reconstruction.

Comparing our reconstruction with the standard one, we first stress the enhancement in resolution (this feature is not immediately visible in Figs. 6 and 7 on account of the interpolation done for presentation purposes) which is more than doubled in each subsection of the pillar (see the Table). As a consequence there is a better ability to delineate the profiles of single quoins. This is more evident in the 2-D reconstruction which shows details not present in the classical reconstruction.

It is worthy of note that we have not used any specific notions on properties of the survey structure, such as mechanical of geophysical properties of the travertine stones under the given solicitation: in fact ours is a "blind reconstruction", and the only constraint posed on the data is the Markov structure of the field. Obviously the results could be improved by using specific ideas that a geophysicist could derive from other forms of inspection and from experience.

CONCLUSIONS

The use of statistical constraints allows a tomographic reconstruction with much better resolution than classical ones. The Markov field, adopted as model for the survey field, has been shown very useful despite its simple form. The drawback is the computation time, intrinsically long on account of the statistical procedure of relaxation; this drawback can be partially avoided by using a parallel implementation of the algorithm.

The use of the statistical method is useful when the resolution obtained with other methods is not sufficient, or alternatively, when the cost of single projections suggests a reduction in their number but a resolution loss is undesirable.

REFERENCES

Besag J.; 1974: *Spatial interaction and the statistical analysis of lattice systems.* J. Royal Static. Soc., series B, **36**, 192-326.

Bernabini M., Cancaniccia M. and Cardarelli E.; 1990: *Seismic survey of some pillars of Coliseum.* Archaeometry.

Cardarelli E.; 1995: *Tomography 3D: a survey on some pillars of Coliseum*. Boll. Geof. Teor. Appl., **37**, 257-265.

Geman D.; 1988: *Random fields and inverse problems in imaging.* Ecole d'Eté de Probabilités de Saint-Flour XVIII Lecture Notes in Mathematics n. 1427, Springer Verlag.

Geman S. and Geman D.; 1984: *Stochastic relaxation, Gibbs distribution, and the Bayesan restoration of images.* IEEE Trans. Pattern Anal. Machine Intell., **PAMI-6**, 721-741.

Paige C. and Saunders M.; 1982: *LSQR: An algorithm for sparse linear equations and sparse least squares.* ACM Transactions on Mathematical Software, **8**, 43-71.